Multiple-Point Geostatistical Modeling of Turbidite and Channel Sands, Deepwater Niger Delta

Ebere Benard and Elijah A. Ayolabi
Department of Geosciences, University of Lagos, Nigeria

ABSTRACT

Three dimensional (3D) seismic attributes were used as training image for multiple-point geostatistical modeling of turbidite and channel sands in the inner fold and thrust belt of the deepwater Niger Delta. These turbidite and channel sands have complex depositional geometries. They are difficult to model using variogram-based two-point statistical techniques such as indicator kriging, sequential indicator simulation (SIS) and truncated Gaussian simulation (TGS). However, accurate prediction of reservoir distribution away from well locations in this depositional setting is critical for field development studies and reservoir management. Hence, the goal of this study is to capture facies heterogeneity in multiple dimension for realistic reservoir property distribution and field performance forecast. 3D seismic data, wireline log, core data and conceptual depositional knowledge were combined to model reservoir facies using different geostatistical methods. The seismic data was used as 3D grid property and constrained with wireline logs for inter-well lithofacies and petrophysical property distribution. This study shows that seismic attributes such as envelope, sweetness, reflection intensity and root mean square (RMS) amplitude, serve as better training images for multiple-point geostatistical facies modeling of geometrically complex turbidite and channel reservoir systems.

Keywords: Turbidites; Seismic Attributes; Geostatistics; Training Image; Deepwater; Niger Delta.

INTRODUCTION

Turbidite and deepwater channel facies types constitute technical challenge in exploration, reservoir characterization and deepwater development studies development (Wood, et al., 2000, Adeogba et al., 2005, Corredor et al., 2005, Heino and Davies, 2006). However, lithology sensitive seismic attributes can be used as training images for multiple-point geostatistical modeling of turbidite and channel sands in complex depositional settings. These complex environments of deposition in the thrust and fold belts of the deep offshore Niger Delta are characterized by the interplay of local mud diapirism and isolated sand distribution within separate mini basins (Caers et al.,2001). Consequently, two point geostatistical methods using variogram analysis have not been very efficient in modeling reservoir properties in these depositional settings as a result of complex geometrical facies trends (Strebelle, 2002). This of course have strong implication for sand facies connectivity, volumetric estimation, well placement and field performance forecast.

However, to accurately represent complex geologic features such as turbidite and channel sands, a measure of correlation between multiple spatial locations is required. Hence, the goal of this study is to capture facies heterogeneity in multiple dimension for realistic reservoir property distribution and field performance forecast.

The objectives of this study include to:-

i. determine the most appropriate post-stack seismic attributes for reservoir characterization in the studied area;
ii. investigate the mechanisms of deepwater sedimentation and lithofacies distribution in the area studied;
iii. characterize and model depositional facies in the area under investigation and;
iv. Compare results of seismic attribute-based multiple point geostatistics with two-point variogram and object-based facies modeling techniques.

LOCATION OF STUDY AREA AND GEOLOGICAL SETTING

The field under study is situated within the mud diapir, inner fold and thrust belt of deepwater Niger Delta, at water depth greater than 1000 m (Figure 1).

The area of study covers approximately 600 km2 in areal extent. The geology is very complex, and is characterized by rapid deposition of prograding sands on over-pressured

© Copyright 2019. Nigerian Association of Petroleum Explorationists.
All rights reserved.

The authors wish to thank the Department of Petroleum Resources (DPR), NNPC, SAPETRO, Total, CNOOC, and Petrobras, for providing the research data for this study.

Multiple-Point Geostatistical

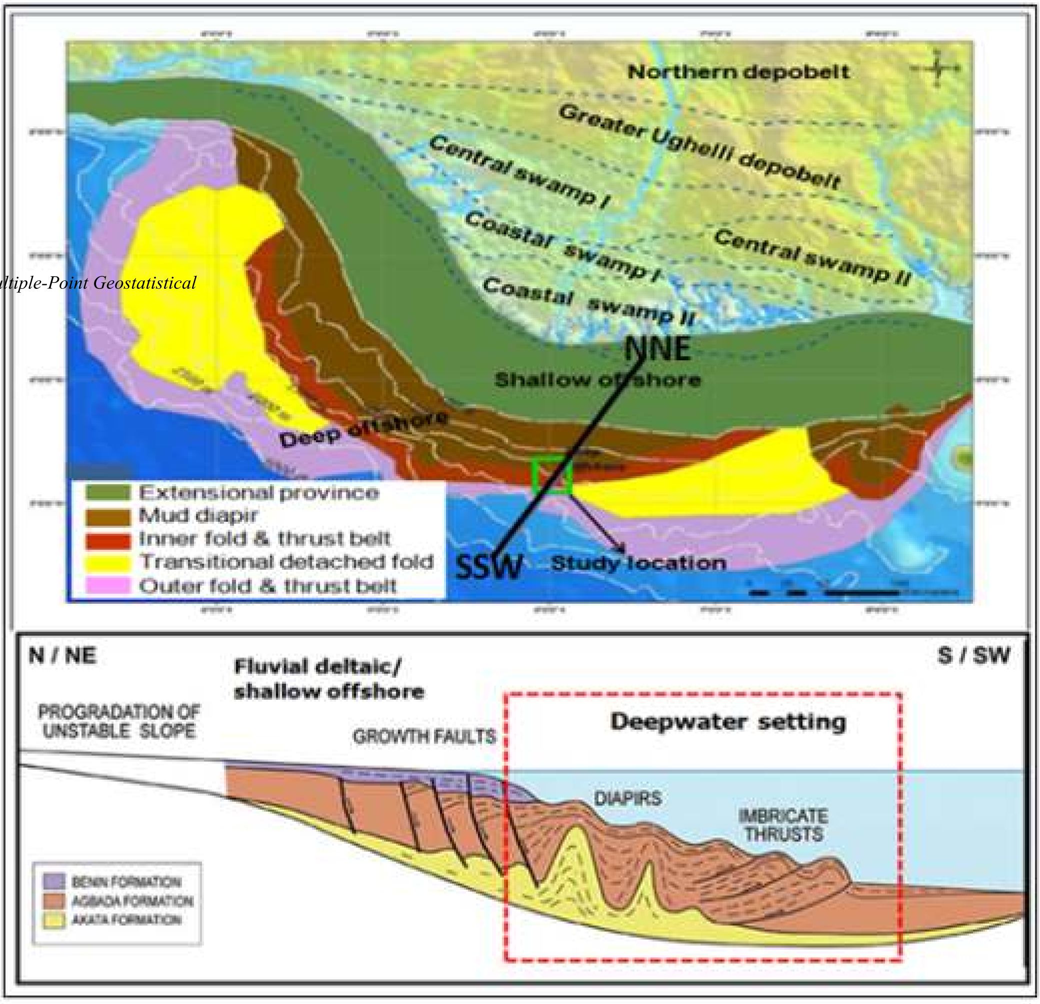

Figure 1: Location of study area (a) Niger Delta Map with study location (b) Cross section showing the deepwater setting.

mobile shale of the Akata Formation. The sedimentary succession of the slope and basin floor deepwater setting, is considered to be dominated by pelagic and hemipelagic marine shales (>80%); with interbedded sandstone deposits of debris flow, turbidite and channel-levee complexes (Graue, 2000).

According to Corredor et al. (2005), the offshore Niger Delta has been subdivided into five structural zones with distinct depositional framework (Figures 1).
These zone include the following:-

i. Extensional province: This zone lies beneath the continental shelf and is characterised by both basinward-dipping and counter-regional growth faults, associated rollovers and depocenters.
ii. Mud diapir zone: This is located beneath the upper continental slope, and is characterised by passive, active and reactive mud diapirs. The mud diapirs include shale ridges and massifs, shale overhangs, vertical mud diapirs, and interdiapir depocenters.
iii. Inner fold and thrust belt: This zone extends in an actuate path across the center of the offshore delta. It is characterised by basinward verging thrust faults and associated folds. It consist of Tertiary to Holocene deep marine sediments.
iv. Transitional detached fold zone: This zone lies beneath the lower continental slope, and is characterised by large areas of little or no deformation. It is interspersed with large detachment folds above structurally thickened Akata Formation.
v. Outer fold and thrust belt: It consists of northern and southern sections that defines two outer lobes of the delta. It is characterised by both basinward and hinterland-verging thrust faults and associated folds. Growth sedimentation rates are low relative to uplift.

DATA SET AND METHODOLOGY

The data set for this research project include approximately 600 km^2 of processed 3D seismic data and wireline log suites from seven wells, and also core photographs from two wells.

The multiple-point geostatistical technique used in the study is based on the single normal equation simulation (Equation 2).

According to Meyer et al., (2001),

$$\lambda = \frac{Cov[A_k, B]}{Var[B]} \quad \text{...(1)}$$

where λ=weight assigned to neighboring value, Cov=covariance, Var= variance, A_k= binary random variable, B=conditioning data event (binary random variable constituted by the n conditioning data).

$$B = \begin{cases} 1 & \text{if } S(u_\alpha)=s_\alpha,\ \alpha=1, \ldots, n \\ 0 & \text{if not} \end{cases}$$

A_k=1 if facies class k occur and is 0 elsewhere

Using equation 1, the following conditional probability is derived

$P(A_k=1|B=1)=E[A_k]+\lambda[1E[B]$.................................(2)

where $E[A_k]$ and E[B] are the expected values of discrete random variable (X) and so

$$E[X]=\sum_{i=1}^{n} x_i P[x=1] \quad \text{....................................(3)}$$

E[X]= Expectation value (weighted average outcome of random variables),

xi= the outcome of the random variable X,

P[X=xi] = probability mass function for the ith outcome,

n-number of possible outcome.

By combining equations 1 and 2, the Bayes' rule is defined in equations 4 to 6.

$P(A_k=1|B=1)$

$$= E_k[A] + \frac{E[A_k B] - E[A_k]E[B]}{E[B]} \quad \text{................(4)}$$

$$P(A_k=1 | B=1)= \frac{P(A_k=1, B=1)}{P(B=1)} \quad \text{................(5)}$$

$$P(A_k=1 | B=1)= \frac{P(B | A_k=1)P(B=1)}{P(B=1)} \quad \text{.........(6)}$$

The single normal equation simulation uses kriging probability to quantify the joint dependency between a random binary variable (A_k) and random variable events (S_u) describing facies classes at grid locations (U_k). For this study volume seismic attributes were generated and used as training image to define random binary variables as seismic facies classes and their corresponding conditional probability of occurrence at every grid cell. The probability volumes were then used as input for the multiple-point geostatistical modeling of the turbidite and channel facies.

Seismic horizons were calibrated with well logs and mapped over the reservoirs of interest across the study area. The resultant structural maps were used to build simple 3D grid framework for reservoir property re-sampling. Generated seismic attributes volumes, lithology logs, petrophysical and elastic rock property logs were then re-sampled and upscaled respectively into the 3D grid. The seismic attribute volumes were visually inspected for architectural patterns and subsequently cross plotted as synthetic logs with elastic rock properties. Seismic attributes with geometrical patterns similar to analog geobodies, and having high correlation coefficients with elastic rock properties were identified. These set of attributes were used to define discrete seismic facies classes and their corresponding probabilities using neural network.

The classified facies probabilities were then assigned lithofacies from the upscaled lithology logs. Also, using variogram analysis the upscaled lithofacies from the well logs were modeled across the field with indicator kriging, sequential indicator simulation and truncated Gaussian simulation techniques respectively. The resultant facies models were compared with the results of the multiple-point geostatistical algorithms. Finally, sedimentological facies analysis from core, logs, and conceptual models were used to validate the geometrical patterns and facies architecture of the modeled turbidite and channel sands.

RESULTS

Multi-attribute Seismic Analysis

Qualitative and quantitative analysis revealed the following seismic attributes : instantaneous amplitude, sweetness, RMS amplitude and reflection intensity as being diagnostic in discriminating between high porosity sand facies from shale prone facies in the fold and thrust belt of the deepwater Niger Delta.

These attributes are characterized by curvilinear geometrical patterns on plan view and have high correlation coefficients of 0.66 to 0.8 in the elastic rock property cross plots (Table 1). In the other hand, instantaneous phase, instantaneous frequency, and relative acoustic impedance having low correlation coefficients are unable to discriminate lithofacies in the study area.

Table 1: Seismic attributes and elastic rock property correlation

Seismic Attribute Versus Rock Properties cross plots	Clean Sand (Correlation Coefficient)	Shaly Sand (Correlation Coefficient)
Sweetness- Young modulus	0.76	0.63
Sweetness- Mu-rho	0.76	0.69
Sweetness- Lambda-rho	-0.68	-0.46
Sweetness - Vp/Vs	-0.73	-0.65
Sweetness - Poisson's ratio	-0.76	-0.64
Acoustic impedance- Young modulus	0.42	0.29
Acoustic impedance- Mu-rho	0.45	0.4
Acoustic impedance- Lambda-rho	-0.36	-0.25
Acoustic impedance- Vp/Vs	-0.46	-0.45
Acoustic impedance - Poisson's ratio	-0.45	-0.37

shale (Figures 3 and 5). These facies models are better adapted to petrophysical property distribution as shown in Figure 6. Alternatively, the resultant facies models from the indicator kriging, sequential indicator simulation and truncated Gaussian simulation facies realization all produced non-unique geologic patterns and architecture in the study area (Figure 4).

Sedimentological Analysis and Architectural Facies Element

Sea floor depositional analogs, gamma ray log, core sedimentological analysis, and lithofacies model reveal sandstone and shale as the two main lithofacies type in the study area; deposited by gravity related processes such as slumping, sliding, debris flow and turbidity current flow (Figures 5, 7, 8 and 9). Figure 5 shows submarine fan and sinuous channels in the present day sea floor. The gamma ray logs generally show cylinderical motif typical of amalgamated channel-lobe reservoir systems as shown in figure 8. Typical sedimentary features on core such as normal grading, inverse grading, parallel lamination, mudclast, sand injectite are all indicative of rapid sedimentation and deposition of sandstones over diapiric shales in a deepwater environment.

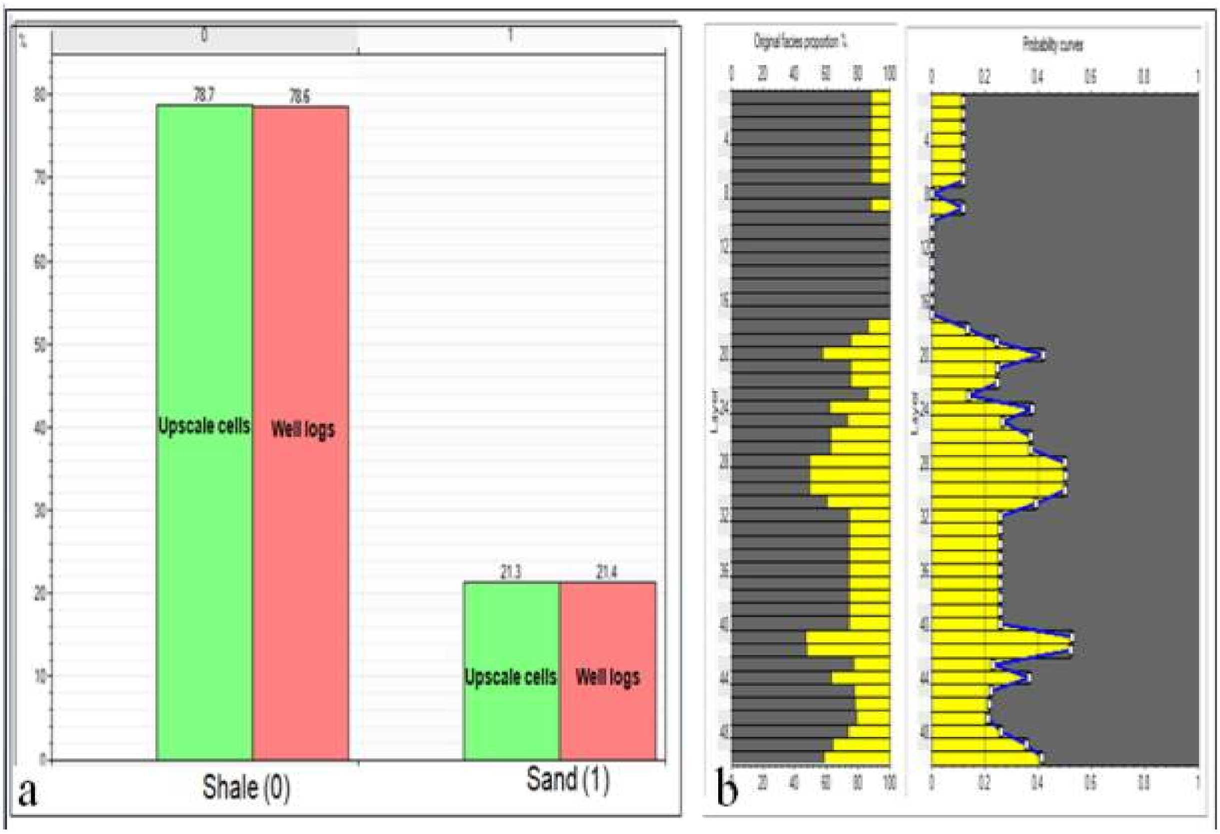

Figure 2: (a) Lithofacies histogram and (b) Facies proportion curve.

Comparing Mulitiple-Point and Two-Point Geostatistical Facies Models

Upscaled lithofacies revealed the global facies proprotion for sand and shale as 79% and 21% respectively in the study area (Figure 2). However, the multiple-point facies models are characterized by lobate fan architecture and sinuous channel morphology interspersed in background

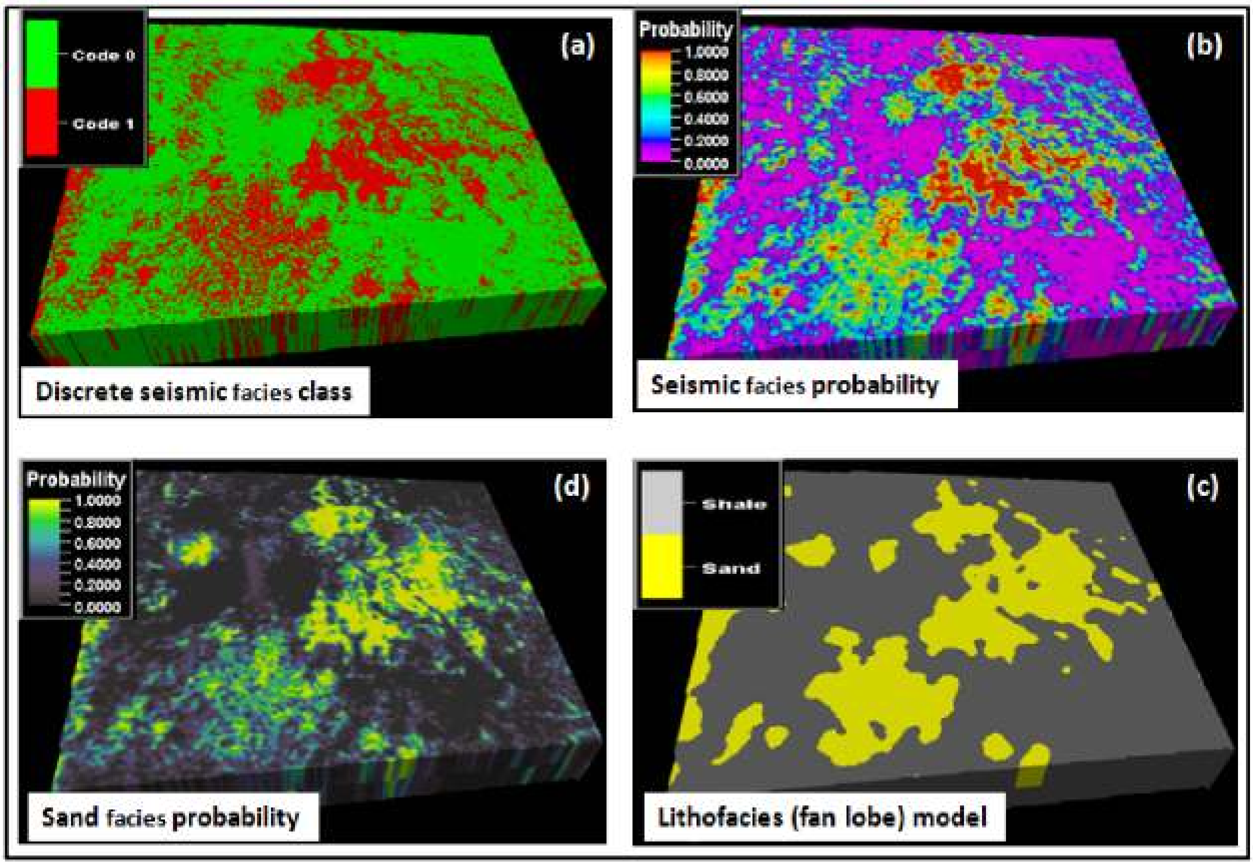

Figure 3: Discrete seismic facies classes, property probability and lithofacies model.

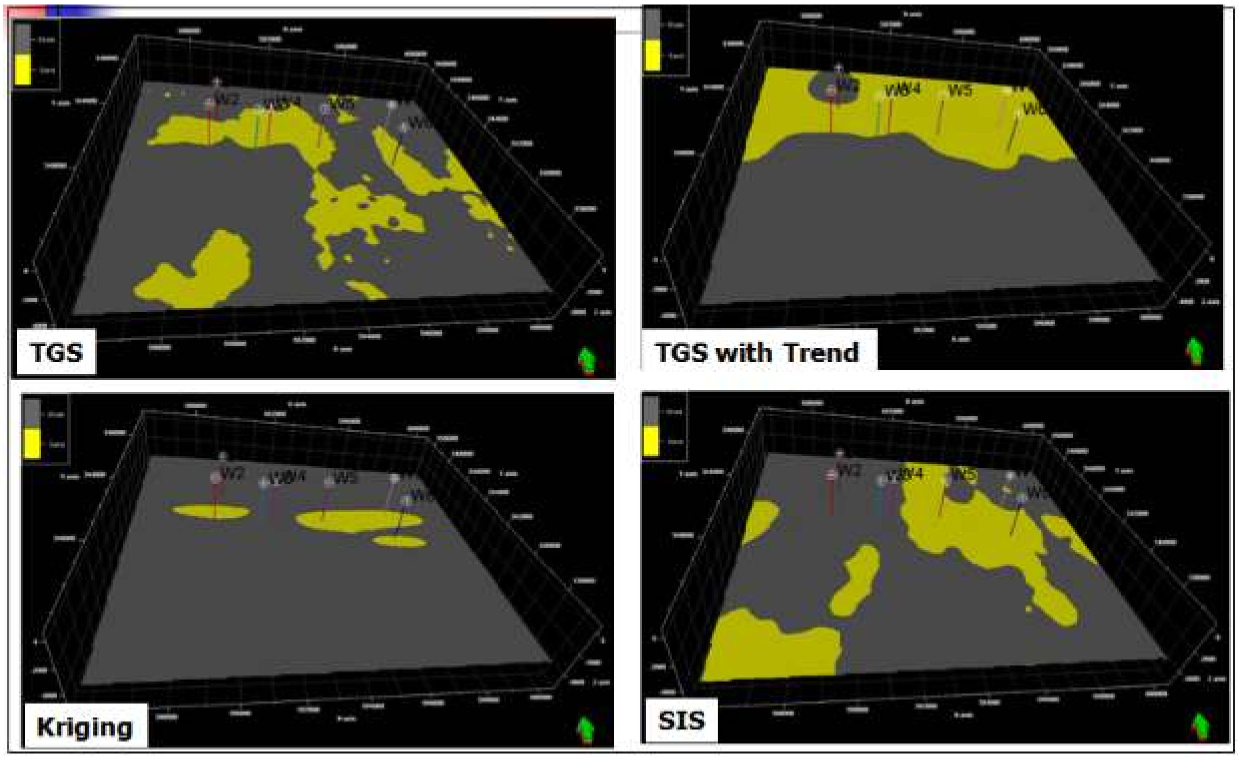

Figure 4: Two-point geostatistical facies models with variogram.

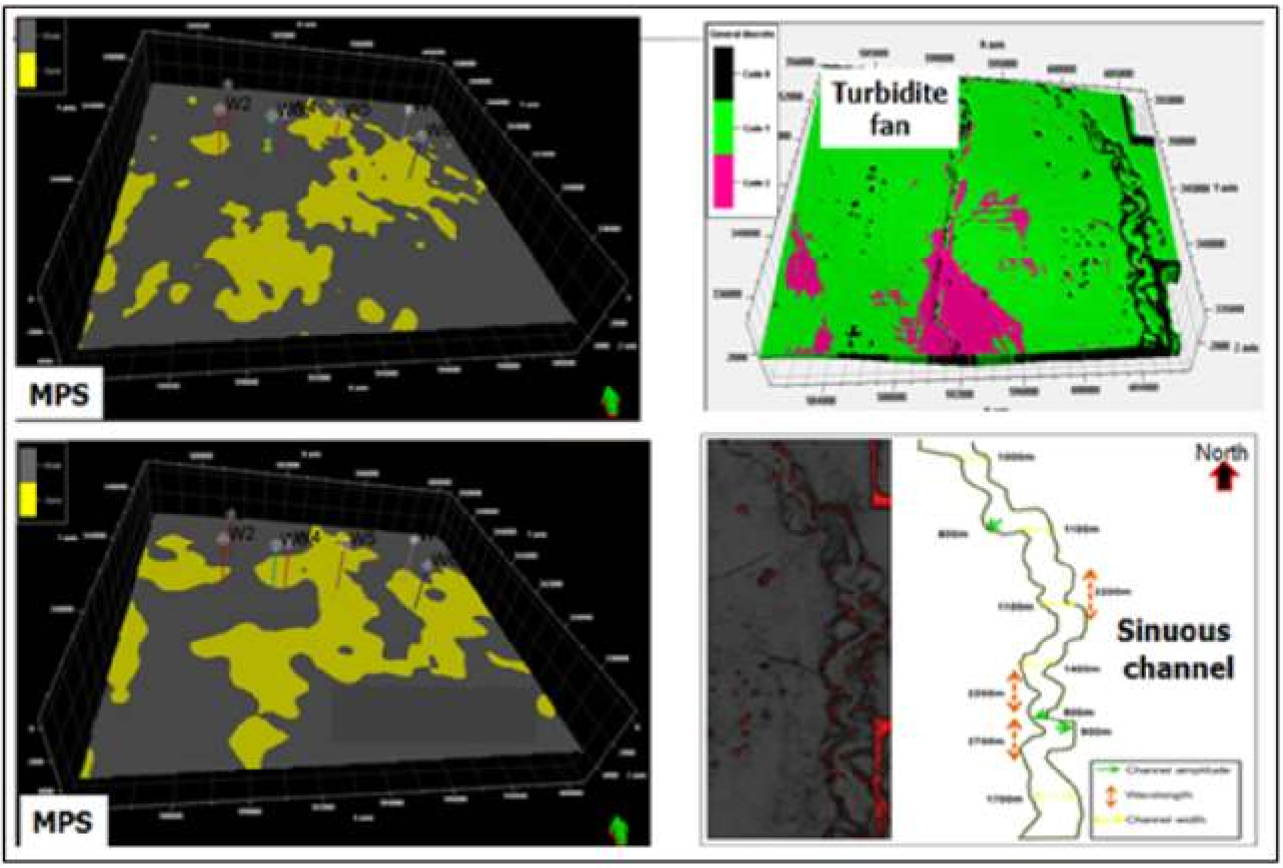

Figure 5: Lobate fan and curvilinear channel facies using multiple-point geostatistical method.

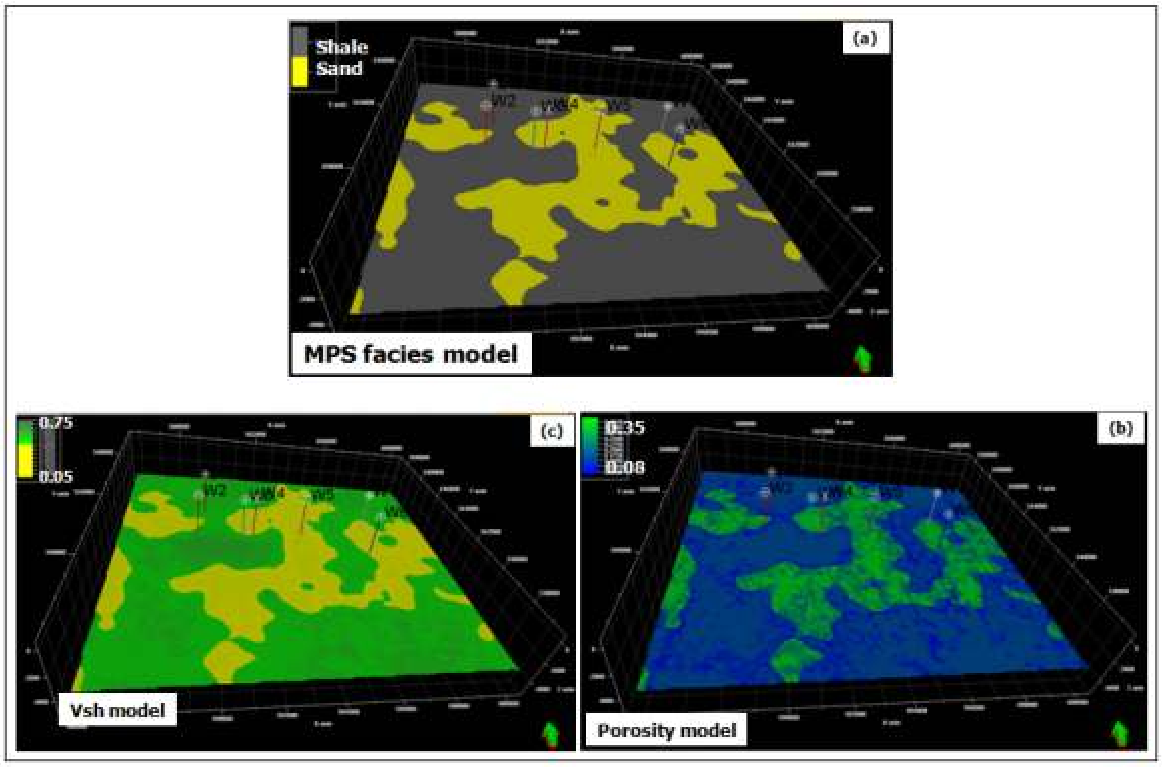

Figure 6: Lithofacies and petrophysical facies models.

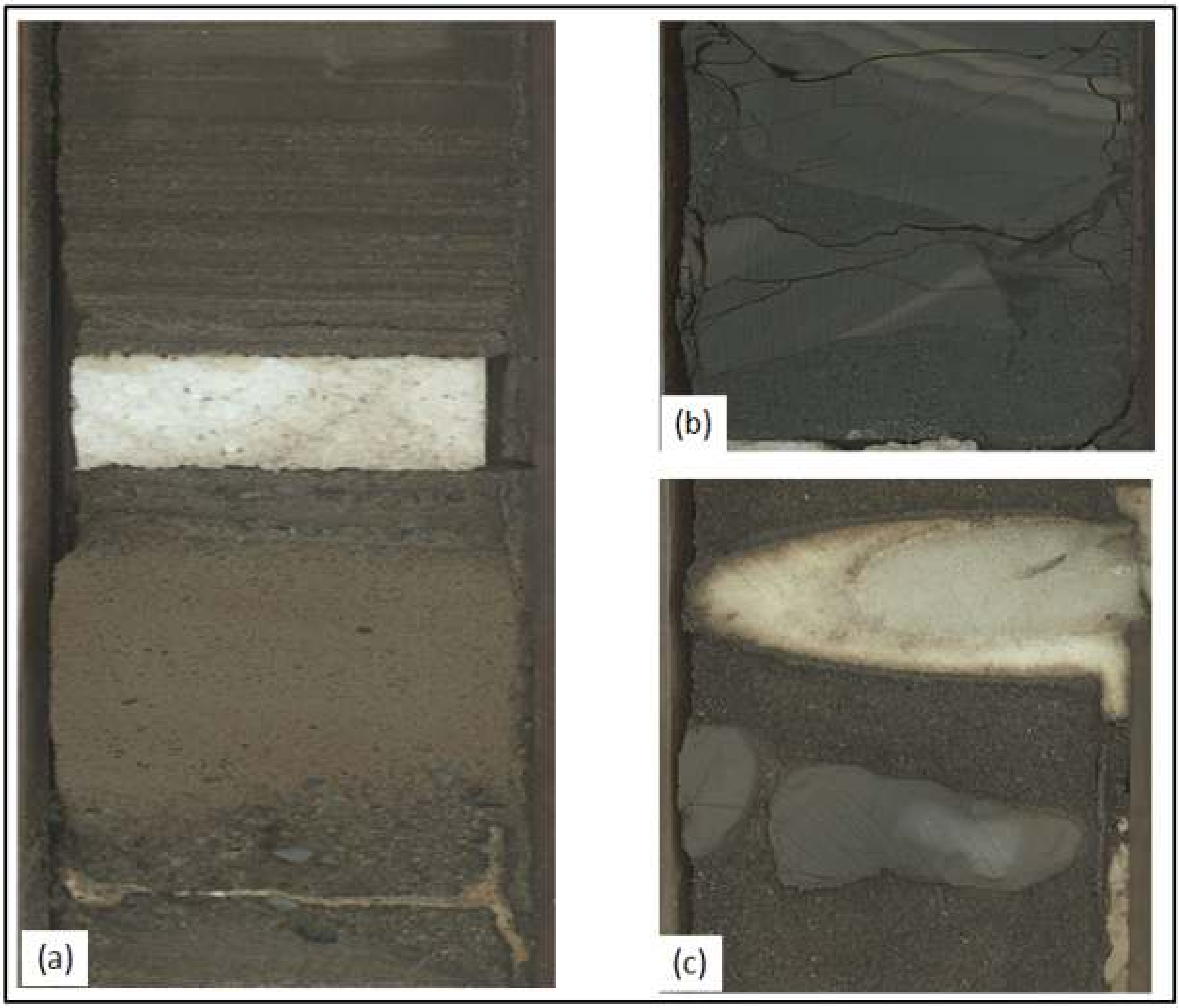

Figure 8: Sedimentological description of core and depositional facies.

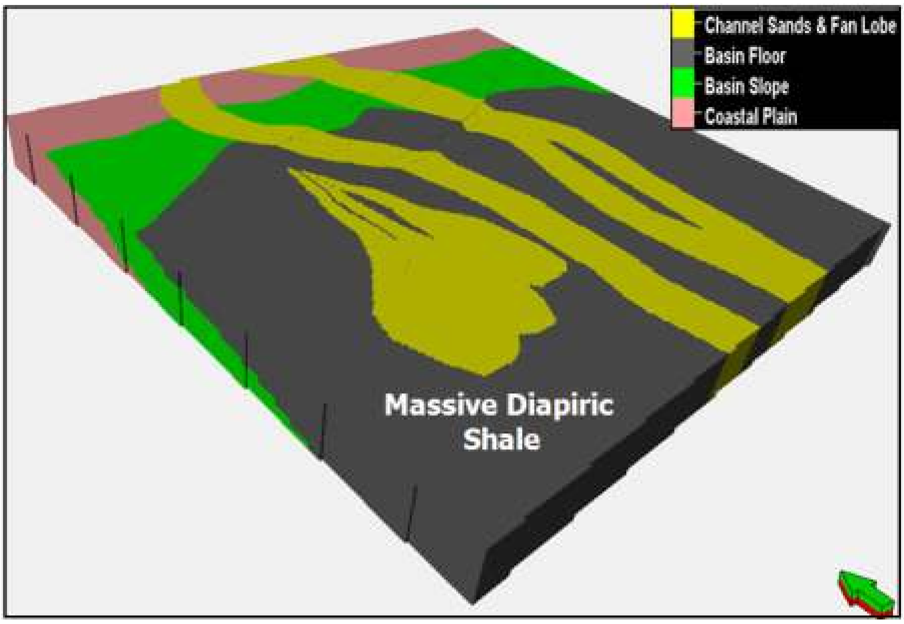

Figure 9: Deepwater Niger Delta conceptual model.

DISCUSSION OF RESULTS

Geostatistical data analysis and histogram of the seven wells give the lithofacies proportion of shale and sand as 79 % and 21 % respectively in the study area (Figure 2). Visual inspection of modeled facies architecture of the different geostatistical algorithms including, indicator kriging, SIS, TGS and seismic attribute-based multiple geostatistical technique (Figures 3 and 4), has revealed the use of 3D seismic attributes as most realistic in reproducing geologic pattern in geometrically complex depositional environments such as the study area. Hence, the integration of 3D seismic attribute as training image for facies modeling, is very effective as multiple point geostatistical property and as complimentary hybrid inputs for inter-well variogram estimation of reservoir properties.

CONCLUSIONS

The integrated approach of multiple-point geostatistical modeling used in this study has improved inter-well lithofacies prediction of turbidite and channel sands. The following seismic attributes: instantaneous amplitude, sweetness, RMS amplitude and reflection intensity are diagnostic for reservoir characterisation and effective as training image for geostatistical facies modeling. The mechanism of sedimentation in the study area are interpreted to include: sediment sliding, slumping, debris flow, turbidity current flow, and hemipelagic settling. The sandstone facies have good reservoir quality and are deposited as amalgamated channel sands and turbidite lobes interspersed over local shale diapirs. Comparatively, the use of seismic attributes as training image for multiple-point facies modeling give better facies and property distribution than the use of variogram in the study area.

REFERENCES CITED

Adeogba, A. A., McHargue, T. R. and Graham, S. A. (2005). Transient fan architecture and depositional controls from near-surface 3-D seismic data, Niger Delta continental slope: AAPG Bulletin, v. 89, p.627–638.

Caers, J, Avseth P, and Mukerji T, (2001). Geostatistical integration of rock physics, seismic amplitudes, and geologic models in North Sea turbidite

Corredor, F., Shaw, J.H and Bilotti F. (2005). Structural Styles in the deep-water fold and thrust belts of the Niger Delta. AAPG Bulletin, v. 89, NO.6 (June 2005), pp 753-780.

Graue, k. (2000). Mud volcanoe in deepwater Nigeria: Marine and Petroleum Geology 17 (2000) 959–974.

Heinio, P., and Davies, R. J. (2006,). Degradation of compressive fold belts, Deepwater Niger Delta. AAPG Bulletin, v. 90, No. 5, p. 753-770.

Meyer, E. Douglas, Elizabeth L. Harvey, Terra E. Bulloch, Jennifer C. Voncannon and Tatun M. Sheffied, (2001). Use of seismic attributes in 3-D geovolume interpretation, The Leading Edge. 1377-1380.

Strebelle, S. (2002). Conditional Simulation of Complex Geological Structures Using Multiple-Point Statistics, Mathematical Geology, Vol. 34, No. 1. p.1-21.

Wood, J. L., Daniel, P. and Ben S, (2000). Seismic attribute and sequence stratigraphic integration methods for resolving reservoir geometry in San Jorge Basin, Argentina: The Leading Edge, p. 952-962.